

# Tumor invasiveness defined by IASLC/ATS/ERS classification of ground-glass nodules can be predicted by quantitative CT parameters

Qian-Jun Zhou<sup>1</sup>, Zhi-Chun Zheng<sup>2</sup>, Yong-Qiao Zhu<sup>1</sup>, Pei-Ji Lu<sup>1</sup>, Jia Huang<sup>1</sup>, Jian-Ding Ye<sup>2</sup>, Jie Zhang<sup>3</sup>, Shun Lu<sup>1</sup>, Qing-Quan Luo<sup>1</sup>

<sup>1</sup>Shanghai Lung Cancer Center, <sup>2</sup>Department of Radiology, <sup>3</sup>Department of Pathology, Shanghai Chest Hospital, Shanghai Jiao Tong University School of Medicine (SJTUSM), Shanghai 200030, China

*Contributions:* (I) Conception and design: QJ Zhou, QQ Luo, S Lu; (II) Administrative support: JD Ye, J Zhang, S Lu; (III) Provision of study materials or patients: YQ Zhu, PJ Lu, J Huang; (IV) Collection and assembly of data: QJ Zhou, ZC Zheng; (V) Data analysis and interpretation: QJ Zhou, QQ Luo; (VI) Manuscript writing: All authors; (VII) Final approval of manuscript: All authors.

*Correspondence to:* Qing Quan Luo. Shanghai Lung Cancer Center, School of Medicine, Shanghai Chest Hospital, Shanghai Jiao Tong University, Shanghai, China. Email: luqingquan@hotmail.com.

**Background:** To investigate the potential value of CT parameters to differentiate ground-glass nodules between noninvasive adenocarcinoma and invasive pulmonary adenocarcinoma (IPA) as defined by IASLC/ATS/ERS classification.

**Methods:** We retrospectively reviewed 211 patients with pathologically proved stage 0-IA lung adenocarcinoma which appeared as subsolid nodules, from January 2012 to January 2013 including 137 pure ground glass nodules (pGGNs) and 74 part-solid nodules (PSNs). Pathological data was classified under the 2011 IASLC/ATS/ERS classification. Both quantitative and qualitative CT parameters were used to determine the tumor invasiveness between noninvasive adenocarcinomas and IPAs.

**Results:** There were 154 noninvasive adenocarcinomas and 57 IPAs. In pGGNs, CT size and area, one-dimensional mean CT value and bubble lucency were significantly different between noninvasive adenocarcinomas and IPAs on univariate analysis. Multivariate regression and ROC analysis revealed that CT size and one-dimensional mean CT value were predictive of noninvasive adenocarcinomas compared to IPAs. Optimal cutoff value was 13.60 mm (sensitivity, 75.0%; specificity, 99.6%), and -583.60 HU (sensitivity, 68.8%; specificity, 66.9%). In PSNs, there were significant differences in CT size and area, solid component area, solid proportion, one-dimensional mean and maximum CT value, three-dimensional (3D) mean CT value between noninvasive adenocarcinomas and IPAs on univariate analysis. Multivariate and ROC analysis showed that CT size and 3D mean CT value were significantly differentiators. Optimal cutoff value was 19.64 mm (sensitivity, 53.7%; specificity, 93.9%), -571.63 HU (sensitivity, 85.4%; specificity, 75.8%).

**Conclusions:** For pGGNs, CT size and one-dimensional mean CT value are determinants for tumor invasiveness. For PSNs, tumor invasiveness can be predicted by CT size and 3D mean CT value.

**Keywords:** Lung cancer; adenocarcinoma; multidetector CT; tumor invasiveness; ground-glass nodule; subsolid nodule

Submitted Oct 07, 2016. Accepted for publication Feb 08, 2017.

doi: 10.21037/jtd.2017.03.170

View this article at: <http://dx.doi.org/10.21037/jtd.2017.03.170>

## Introduction

Advances of technology in computed tomography (CT) have significantly increased the detection of early stage lung cancers with subsolid nodules on CT scans (1), which can be further classified as pure ground glass nodules (pGGNs) or part-solid nodules (PSNs) (2).

The International Association for the Study of Lung Cancer, American Thoracic Society and European Respiratory Society (IASLC/ATS/ERS) proposed a new pathology classification of lung adenocarcinoma in 2011, which represents the evolving advances in stratifying lung adenocarcinoma based on tumor morphology (3). A relationship between CT findings and pathology was observed that the ground glass portion of subsolid nodule correlated to the noninvasiveness of lung adenocarcinoma. However, the majority of these researches was based on the Noguchi classification or 2004 WHO classification (4,5). Several studies using 2011IASLC/ATS/ERS classification focused on the differentiation of atypical adenomatous hyperplasia (AAH) from invasive pulmonary adenocarcinoma (IPA) (6), or differentiation of preinvasive lesion (AAH and AIS) from IPA via visual inspection of nodule features and linear measurements (7). Thus, it is still challenging for surgeons to correctly judge the invasiveness of subsolid nodules with objective and reliable parameters, rendering determining optimal procedure and the appropriate timing for surgical intervention.

Development of multidetector CT (MDCT) and computer technology have made quantitative image analysis possible for subsolid nodules. The goal of this study is to investigate the value of employing differentiating CT parameters, including quantitative and qualitative, to differentiate noninvasive pulmonary adenocarcinomas from IPAs by analyzing subsolid nodules retrospectively.

## Methods

### Patients

This study was approved by the Ethics Committee of the Shanghai Chest Hospital, and the patients' written informed consent was waived by the Ethics Committee. From January 2012 to January 2013, a total of 679 resected and pathologically proved stage 0-I lung adenocarcinoma patients were in our center. Thereafter, multiple lung adenocarcinomas; solid lesion on CT scan; lesions <5 mm or >3 cm on CT scan were excluded. Finally, 211 patients with a single lung adenocarcinoma (5 mm < T < 3 cm)

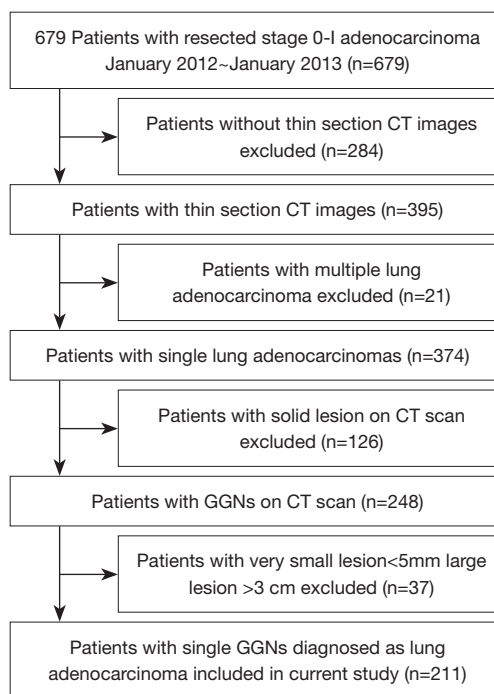


**Figure 1** Flowchart of patient selection. Numbers in parentheses are numbers of patients.

whose MDCT scans appeared as subsolid nodules were included (*Figure 1*). All patients were not preoperatively treated with chemotherapy or radiotherapy, 56 were men (mean age, 55.18±10.06 years; range, 29–80) and 155 were women (mean age, 54.74±9.41 years; range, 30–74 years). Histopathology was based on the 2011IASLC/ATS/ERS classification of lung adenocarcinoma. In this study, adenocarcinoma in situ (AIS) and minimally invasive adenocarcinoma (MIA) were defined as noninvasive adenocarcinoma (8), and IPAs were defined as invasive adenocarcinoma including lepidic predominant, acinar predominant, papillary predominant and other subtypes.

### CT examination

Unenhanced helical CT scans were performed with a 64-detector row scanner (Brilliance, Philips, Cleveland, USA). The parameters of routine CT were as follows: detector collimation, 0.625 mm × 64; pitch, 1.08; 120 kV and 250 mA; 5–7 s scan time; SFOV, 400 mm; section thickness and interval, 5.0 and 5.0 mm; filter function C, DFOV, 363 mm; matrix, 512×512. When a lung nodule was found, a HRCT target scan was performed by the same CT scanner

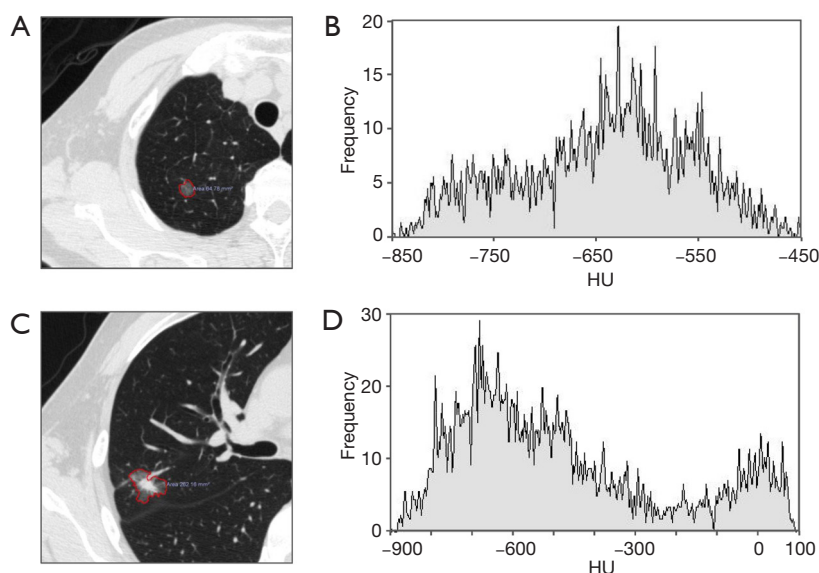


**Figure 2** One-dimensional mean CT value on axial section of pGGN and PSN. (A) CT image of a 10-mm pGGN in the right upper lobe of a 71-year-old woman in which the nodule was confirmed as AIS by VATS extended wedge resection; (C) its one-dimensional mean CT value was  $-647$  HU on axial section; (B) CT image of a 25-mm PSN in the right upper lobe of a 51-year-old man in which the nodule was diagnosed as IPA by VATS lobectomy; (D) its one-dimensional mean CT value was  $-482$  HU on axial section, maximum CT value was  $77$  HU.

with following parameters: collimation,  $0.625\text{ mm} \times 64$ ; pitch,  $0.64$ ,  $120\text{ kV}$  and  $300\text{ mA}$ ;  $1\text{--}3\text{ s}$  scan time; SFOV,  $180\text{ mm}$ ; section thickness and interval,  $1.0$  and  $0.5\text{ mm}$ , range  $5\text{ cm}$ ; filter function F, DFOV,  $180\text{ mm}$ ; matrix,  $1,024 \times 1,024$ . Images were reconstructed by “standard” and “sharp” algorithms for routine CT and targeted HRCT scans respectively. Analysis of CT density was conducted by a computer graphics support system (Tivew software, WinningSoft, Shanghai, China).

### Evaluation of CT features

Two chest radiologists (Z.Z.C., and Y.J.D., with 15 and 31 years of experience in chest imaging, respectively), blinded to the histological results, assessed CT images on lung windows (level,  $-520\text{ HU}$ ; width,  $1,450\text{ HU}$ ). The average values of quantitative parameters including CT size, area and CT value measured by two radiologists were applied for analysis. When discrepancies of morphological parameters of two radiologists occurred, decisions were reached by consensus. All subsolid nodules were classified as pGGN or PSN. pGGN was defined as a shadow completely occupied by a hazy increased attenuation of the lung, with reservation of the bronchial and vascular margins in the lesion with no solid regions. PSN was

defined as a heterogeneous attenuation with an internal solid component completely obscuring the underlying lung parenchyma. The normal structures such as vessels and bronchioli within or around the nodule were eliminated manually when performing CT value analyzing. CT findings of each lesion were analyzed as follows: (I) one-dimensional mean CT value (attenuation values of pGGN and PSN, manually indicating the border of the biggest area of interest on axial section with subsequent quantitative analysis by computer program) (Figure 2); (II) maximum CT value (for PSN, the maximum attenuation values within the border of the biggest area of the nodule on axial section); (III) three dimensional (3D) CT value (for PSN, mean CT value of the biggest area of interest of axial, coronal and sagittal section were measured, the average value of the three sections was the 3D CT value) (Figure 3); (IV) location; (V) multiplicity (solitary, multiple); (VI) size (the largest diameter on axial section); (VII) area; (VIII) solid component area (for PSN, the largest solid component area on axial section); (IX) solid proportion (for PSN, dividing the solid component area by the lesion area); (X) margin (spiculated, nonspiculated); (XI) border (lobulated, nonlobulated); (XII) bubble lucency; (XIII) pleural indentation; (XIV) vascular change (dilated, rigid, convergent and tortuous); and (XV) spinous protuberance.

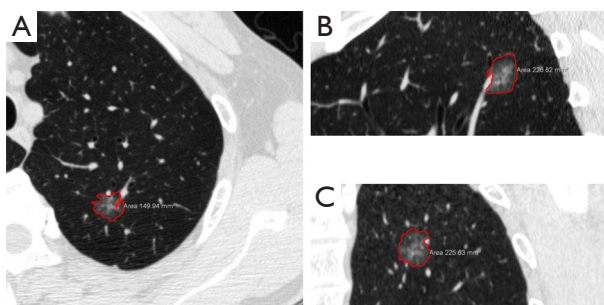


**Figure 3** CT image of a 15-mm PSN in the left upper lobe of a 58-year-old man in which the nodule was diagnosed as MIA by VATS lobectomy, and its 3D mean CT value was  $-655$  HU. (A) Axial view of the lesion, mean CT value was  $-674$  HU; (B) coronal view of the lesion, mean CT value was  $-667$  HU; (C) sagittal view of the lesion, mean CT value was  $-625$  HU.

### Statistical analysis

pGGN and PSN were separated to perform statistical analysis. Patients' sex and CT qualitative features between noninvasive and invasive adenocarcinoma were compared by Pearson  $\chi^2$  or Fisher exact test. Patients' age, pT size and CT quantitative parameters were compared by using unpaired *t*-test. The optimal cut-off values were calculated by receiver operating characteristic (ROC) curve analysis. Multiple logistic regression analysis was conducted to ascertain which factors differentiate noninvasive adenocarcinoma from IPA, and the parameters with  $P < 0.10$  were input as variables. Weighted  $k$  statistic was used to test the interobserver agreement for qualitative CT findings, and the degree of agreement was according to Landis and Koch (9). Concordance correlation coefficients (CCCs) were calculated for interobserver agreement for measurements of CT size, CT area, solid component area, 1D mean CT value, 3D mean CT value, 1D maximum CT value. Statistical analysis was performed by using SPSS, version 19.0 (SPSS, Chicago, IL, USA). A *P* value of less than 0.05 was considered statistically significant.

### Results

Clinical and pathological features were listed in *Table 1*. There were no significant differences in demographic findings between noninvasive adenocarcinomas and IPAs appearing as pGGN or PSN. The pathological size of lesion was significantly smaller in noninvasive adenocarcinomas compared to IPAs in both pGGO and PSN.

### CT features of pGGNs

Noninvasive adenocarcinomas were significantly smaller in CT size ( $P=0.002$ ) and CT area ( $P=0.014$ ). One-dimensional mean CT value was significantly lower in noninvasive adenocarcinomas ( $P=0.004$ ). The presence of bubble lucency was significantly less frequent in noninvasive adenocarcinomas in comparison to IPAs ( $P=0.011$ ). Other morphologic features were not significantly different between noninvasive adenocarcinomas and IPAs. *Tables 2,3* summarized the differentiating CT features between noninvasive adenocarcinomas and IPAs appearing as pGGNs. There was only one patient diagnosed as IPA with pGGN less than 10 mm, whose CT size and CT value is 6.89 mm and  $-515.85$  Hu, respectively.

### ROC analysis and multiple logistic regression of pGGNs

ROC analysis demonstrated that the area under the ROC curve (AUC) for CT size and CT area was 0.890 (95% confidence interval: 0.780, 1.000) and 0.893 (95% confidence interval: 0.796, 0.991), and the optimal cutoff value of CT size and CT area for differentiating noninvasive adenocarcinomas from IPAs was less than 13.60 mm (sensitivity, 75.0%; specificity, 99.6%) and  $82.40 \text{ mm}^2$  (sensitivity 87.5%, specificity 82.9%). AUC for one-dimensional mean CT value is 0.703 (95% confidence interval: 0.565, 0.840), and the optimal cutoff value for differentiating noninvasive adenocarcinomas from IPAs was less than  $-583.60$  HU (sensitivity, 68.8%; specificity, 66.9%) (*Figure 4*).

Because CT size was closely correlated to the CT area, the CT area was removed from the multiple regression analysis. CT size, one-dimensional mean CT value, lesion margin, bubble lucency and vascular sign were input as independent variables for multivariate analysis. Multivariate regression revealed that CT size ( $P=0.000$ ; 95% confidence interval: 1.336, 2.282; odds ratio, 1.746) and one-dimensional mean CT value ( $P=0.010$ ; 95% confidence interval: 1.002, 1.017; odds ratio, 1.010) were the predictive factors of noninvasive adenocarcinomas compared to IPAs (*Table 4*). The *P* values of lesion margin, bubble lucency and vascular change were 0.996, 0.731, 0.533, respectively.

### CT features of PSNs

Among the CT features, noninvasive adenocarcinomas were significantly smaller in CT size: ( $P < 0.001$ ), and

**Table 1** Characteristics of patients

Characteristics	AIS (n=79)	MIA (n=75)	Noninvasive (n=154)	IPA (n=57)	P value (noninvasive vs. IPA)
pGGN (n=137)	n=71	n=50	n=121	n=16	
Age (y)	51.70±10.00	54.30±9.76	52.61±9.94	55.19±7.69	0.320
Sex					
Male	17	8	25	5	0.343
Female	54	42	96	11	
pT size (mm)	6.7±1.9	8.0±2.7	7.2±2.0	13.1±5.5	<0.001
Surgical procedure					
Lobectomy	46	40	86	15	0.069
Sublobar resection	25	10	35	1	
PSN (n=74)	n=8	n=25	n=33	n=41	
Age (y)	54.37±12.01	60.04±6.00	58.67±8.04	58.27±8.44	0.837
Sex					
Male	6	7	13	13	0.491
Female	2	18	20	28	
pT size (mm)	7.9±2.7	10.3±3.3	9.7±3.3	15.7±5.1	<0.001
Surgical procedure					
Lobectomy	5	21	26	38	0.082
Sublobar resection	3	4	7	3	

pGGN, pure ground glass nodule.

CT area ( $P=0.002$ ). Noninvasive adenocarcinomas had significant smaller solid component area ( $P=0.004$ ) and solid proportion ( $P=0.016$ ) in comparison to IPAs. One-dimensional mean CT value ( $P<0.001$ ) and maximum CT value ( $P<0.001$ ), and 3D mean CT value ( $P<0.001$ ) were significantly lower in noninvasive adenocarcinomas. There was no significant difference with regard to morphologic features between noninvasive adenocarcinomas and IPAs. *Tables 2,3* concluded the differentiating CT features between noninvasive adenocarcinomas and IPAs appearing as PSNs.

#### ROC analysis and multiple logistic regression of PSNs

ROC analysis showed that the AUC for CT size and CT area was 0.773 (95% confidence interval: 0.665, 0.880) and 0.789 (95% confidence interval: 0.684, 0.898), and the optimal cutoff value of CT size and CT area for differentiating noninvasive adenocarcinomas from IPAs was less than 19.64 mm (sensitivity, 53.7%; specificity,

93.9%) and 169.93 mm<sup>2</sup> (sensitivity 63.4%, specificity 87.9%), respectively. AUC for solid component area and solid proportion was 0.778 (95% confidence interval: 0.674, 0.880) and 0.652 (95% confidence interval: 0.526, 0.778) respectively. The optimal cutoff value of solid component area and solid proportion for differentiating noninvasive adenocarcinomas from IPAs was less than 19.045 mm<sup>2</sup> (sensitivity, 78.0%; specificity, 66.7%) and 21.365% (sensitivity 53.7%, specificity 81.8%), respectively. AUC for mean CT value and maximum CT value of axial section, and 3D CT value is 0.832 (95% confidence interval: 0.737, 0.928), 0.776 (95% confidence interval: 0.665, 0.888), and 0.860 (95% confidence interval: 0.772, 0.949), respectively. The optimal cutoff value of one-dimensional mean CT value and maximum CT value of axial section, and 3D mean CT value for differentiating noninvasive adenocarcinomas from IPAs was less than -546.13 HU (sensitivity, 75.6%; specificity, 81.8%), -14.00 HU (sensitivity 56.2%, specificity 75.8%), and -571.63 HU (sensitivity, 85.4%; specificity, 75.8%), respectively (*Figure 4*).

**Table 2** CT features of pGGNs (n=137)

Characteristics	Noninvasive adenocarcinoma (n=121)	IPA (n=16)	P value (Noninvasive vs. IPA)
CT size (mm)	9.52±2.51	16.78±7.74	0.002
CT area (mm <sup>2</sup> )	61.70±34.17	162.88±145.30	0.014
Mean CT value (HU)	-613.63±93.05	-541.14±103.39	0.004
Lesion border			0.240
Lobulated	33	7	
Non lobulated	88	9	
Lesion margin			0.120
Spiculated	8	3	
Nonspiculated	113	13	
Spinous process	8	1	1.000
Pleural indentation	18	1	0.699
Bubble lucency	18	7	0.011
Vascular change	80	14	0.083
Location			0.527
Inner	17	4	
Outer	71	8	
Middle	33	4	

Because the CT size was closely correlated to the CT area, and the same relation as solid component area and solid proportion, the CT area and solid component area were removed from the multiple regression analysis. CT size, solid proportion, one-dimensional mean and maximum CT value, 3D mean CT value, lesion border, bubble lucency and vascular change were input as independent variables (*Table 4*). CT size ( $P=0.002$ ; 95% confidence interval: 1.126, 1.742; odds ratio, 1.400) and 3D mean CT value ( $P=0.019$ ; 95% confidence interval: 1.004, 1.040; odds ratio, 1.022) were the significant differentiating factors of noninvasive adenocarcinomas compared to IPAs.

#### ***Interobserver agreement analysis for CT findings of subsolid nodules***

The  $k$  value of qualitative CT morphologic features of subsolid nodules varied between 0.475~0.898. The CCCs for quantitative CT parameters were very high, between 0.892~0.998. *Table 5* summarized the results of interobserver

agreement analysis for CT findings of the subsolid nodules.

## **Discussion**

The imaging description of 2011 IASLC/ATS/ERS entities were insufficient in describing lesions in nature. It was reported that AIS and MIA have a 100% disease-free survival (DFS), which is much lower in IPAs (10,11). Thus, we included AISs and MIAs into the noninvasive adenocarcinomas. The present study studied qualitative and quantitative parameters to determine the CT features to predict the invasiveness of lung adenocarcinoma. Based on our results, quantitative parameters may enable surgeons to predict tumor invasiveness of subsolid nodules to aid in clinical decision-makings pertaining to the timing of surgical intervention and extent of resection.

A recent study reported that tumor invasiveness defined by IASLC/ATS/ERS classification correlated with the 5-year survival data of p-stage IA lung adenocarcinoma (8). In our study, there was significant difference between noninvasive

**Table 3** CT features of and PSNs (n=74)

Characteristics	Noninvasive adenocarcinoma (n=33)	IPA (n=41)	P value (noninvasive vs. IPA)
CT size (mm)	14.74±4.36	20.48±6.63	<0.001
CT area (mm <sup>2</sup> )	123.65±79.74	225.74±133.87	0.002
Solid component area (mm <sup>2</sup> )	17.52±12.26	52.13±52.17	0.004
Solid proportion (%)	15.38±12.42	24.03±16.78	0.016
1D Mean CT value (HU)	-609.05±102.66	-446.60±178.35	<0.001
3D Mean CT value (HU)	-616.05±99.63	-464.70±105.53	<0.001
1D Maximum CT value (HU)	-89.36±108.68	12.07±68.06	<0.001
Lesion border			0.055
Lobulated	21	35	
Nonlobulated	12	6	
Lesion margin			0.748
Spiculated	12	19	
Nonspiculated	21	22	
Spinous process	6	11	0.773
Pleural indentation	13	22	0.222
Bubble lucency	11	22	0.080
Vascular sign	29	40	0.099
Location			0.137
Inner	0	4	
Outer	22	28	
Middle	11	9	

adenocarcinomas and IPAs in CT size and area, one-dimensional mean CT value and bubble lucency in pGGNs. Lim *et al.* found that there was no significant difference among AIS, MIA and IPA with regard to CT size and morphologic features in pGGNs (12). Lee *et al.* reported that CT size and lesion border were significantly different between preinvasive lesions and IPAs in pGGNs (7). The presence of bubble lucency indicated the nodules that grew over an interval of 2 years (13). As for PSNs, we found that CT size and area, solid component area, solid proportion, one-dimensional mean CT and maximum CT value, and 3D mean CT value were significantly different between noninvasive adenocarcinomas and IPAs. In Lee's study, there were significant differences in lesion size, solid proportion

and morphologic features such as lesion margin, border and pleural retraction between preinvasive lesions and IPAs (7). None of the morphologic features was significant with regard to tumor invasiveness for PSNs in present study.

Many radiological studies reported a strong relationship between the degree of GGO and pathology, however, so far there has been no consensus with regard to the best measurement metric to predict the tumor invasiveness and patient survival. Suzuki *et al.* had classified small adenocarcinoma into six subtypes according to GGO extent, however, having only the degree of GGO is insufficient to evaluate all subsolid nodules (14). Tumor disappearance rate (TDR) was also used to examine the

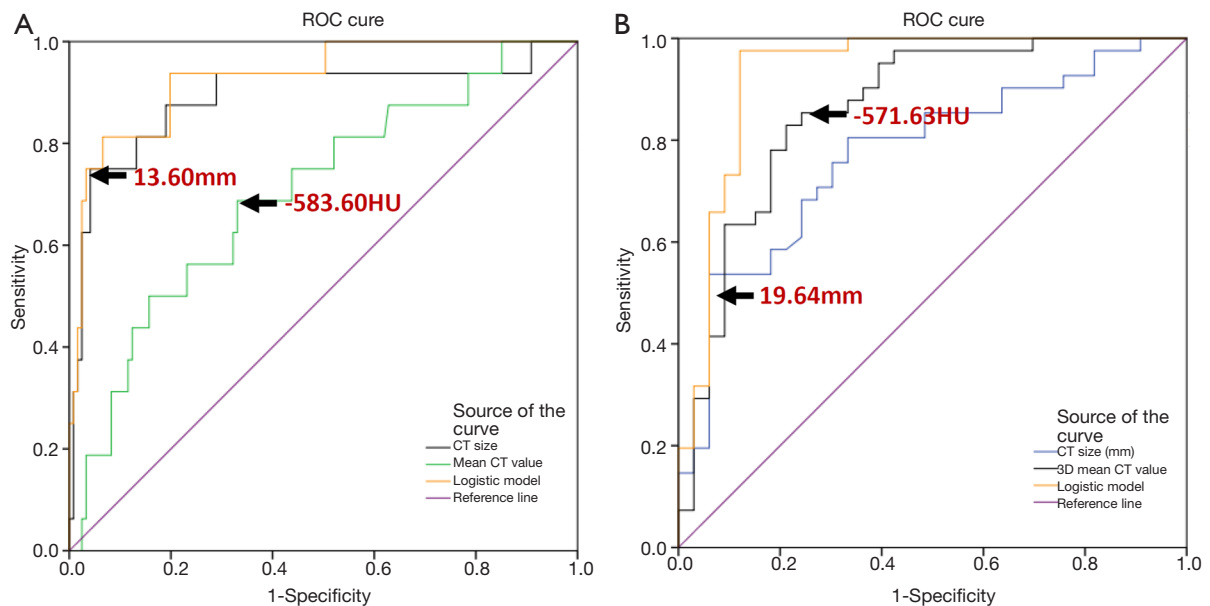


**Figure 4** ROC analysis of pGGN and PSN. (A) ROC curve of the CT size and one-dimensional mean CT value for differentiation between noninvasive adenocarcinoma and IPA for pGGNs, showing cutoff value at 13.60 mm and -583.60 HU; (B) ROC curve of the CT size and 3D mean CT value for differentiation between noninvasive adenocarcinoma and IPA for PSNs, showing cutoff value at 19.64 mm and -571.63 HU.

**Table 4** Logistic regression analysis for CT parameters to differentiate noninvasive adenocarcinomas from IPAs in GGNs

Variable	P value	OR	95% CI for OR
<b>pGGNs</b>			
CT size (mm)	0.000	1.746	1.336–2.282
Mean CT value (HU)	0.010	1.010	1.002–1.017
Bubble lucency	0.731	0.730	0.121–4.399
Vascular sign	0.533	0.533	0.271–12.515
<b>PSNs</b>			
CT size (mm)	0.002	1.400	1.126–1.742
Solid component area (mm <sup>2</sup> )	0.272	0.982	0.951–1.014
1D Mean CT value (HU)	0.835	0.998	0.983–1.014
3D Mean CT value (HU)	0.019	1.022	1.004–1.040
Lesion border	0.494	1.906	0.300–12.131
Bubble lucency	0.723	1.328	0.276–6.399
Vascular sign	0.969	1.061	0.053–21.413

**Table 5** Interobserver agreement analysis for CT findings of subsolid nodules

Variables	CCC	Weighted (k)	95% CI for CCC or k
Nodule type	–	0.898	0.835–0.961
Lesion border	–	0.625	0.521–0.729
Lesion margin	–	0.475	0.338–0.612
Spinous process	–	0.481	0.330–0.632
Pleural indentation	–	0.725	0.623–0.827
Bubble lucency	–	0.529	0.401–0.649
Vascular change	–	0.537	0.414–0.660
CT size	0.998	–	0.996–1.000
CT area	0.997	–	0.991–1.000
Solid component area	0.978	–	0.954–1.000
1D mean CT value	0.988	–	0.984–0.992
3D mean CT value (HU)	0.892	–	0.825–0.959
1D maximum CT value (HU)	0.990	–	0.986–0.994

ratio of solid component by linear measurement of area on mediastinal window and lung window settings (15). In fact, many subsolid nodules were non-discernible on mediastinal window view settings, which made it difficult to use TDR to evaluate such lesions. Morphological parameters appeared to be inconsistent predictors for the pathology of lung adenocarcinoma (16). Therefore, objective and quantitative metrics are needed to analyze subsolid nodules.

Increased CT value is an important predictive factor for tumor invasiveness (1). However, using CT value in the management of GGNs was debated for the influence of different CT protocols such as section thickness and the use of contrast-medium (17). In our study, all the CT images were unenhanced by 1 mm thin section CT (TSCT), which complied with the Fleischner Society guideline's requirement (2). For pGGNs, we chose one-dimensional mean CT value to differentiate the invasiveness due to its homogeneous characteristic (18). The only patient diagnosed as IPA with pGGN under 10 mm, invasiveness could be identified via mean CT value, which was  $-515.85$  HU (cutoff value is  $-583.60$  HU). Two-dimensional and 3D quantitative analysis had been used to evaluate the CT attenuation or CT number based histogram to differentiate among AAH, BAC and IPA (19). Ikeda *et al.* reported that the 3D mean CT value was the more useful for differentiating BAC from IPA (20). For PSNs, we found that using the CT value as a differentiator was better than using CT size with regard to the accuracy of ROC analysis, especially the 3D mean CT value seemed to be with the highest accuracy (sensitivity, 85.4%; specificity, 75.8%).

When and how subsolid lesions should be resected still remained controversial. The size of the lesion alone has been believed not to be an accurate predictive factor of tumor invasiveness (21). We found that mean CT value coupled with CT size were optimal quantitative parameters to predict tumor invasiveness, and the cutoff values in this study were close to previous reports. Suzuki *et al.* suggested that 15 mm was the resection criterion for pGGNs (14). Kitami *et al.* reported the cutoff value of CT size and one-dimensional mean CT value were 10 mm and  $-600$  HU based on Noguchi classification (18). It is reasonable that our results were slightly higher than Kitami's data because we had included MIA into noninvasive adenocarcinoma. The interim guidelines of pulmonary GGNs by Godoy recommended that 10mm or larger is the criterion for surgical resection for pGGNs (22). We suggest that for pGGNs, if the CT size  $>13.60$  mm, and mean CT value  $>-583.60$  HU, surgery (lobectomy) is indicated, because the lesion was highly

diagnosed as IPA. If the CT size of pGGNs is between 10 and 13.60 mm, one-dimensional mean CT value would be a recommendation for treatment strategy. Because there was some overlap between noninvasive and invasive adenocarcinomas with regard to CT features, even for pGGN less than 10 mm, mean CT value will be still critical for the treatment decision. Multivariate logistic analysis also revealed that CT size and 3D mean CT value were predictive of noninvasive adenocarcinomas from IPAs for PSNs, and the cutoff was 19.64 mm and  $-571.63$  HU, respectively. We suggested that the combination of CT size and 3D mean CT number would also be helpful for the surgical procedure options for PSNs (20). Interestingly, although the difference of cutoff value of CT size between pGGNs and PSNs was not small (13.60 *vs.* 19.64 mm), the cutoff value of mean CT value between pGGNs and PSNs was close ( $-583.60$  *vs.*  $-571.63$  HU). Because the diagnosis of GGN is subjective sometime, it is noteworthy that the mean CT value reflecting the true nature of the GGN lesion is critical for the management tactics.

There were several limitations in our study. First, we have not included the benign lesions. However, the operation criteria for GGNs based our results have made us to resect lung adenocarcinoma in 95% patients with GGNs (data not show). Second, 3D mean CT value in this study was "semiautomated", in which we manually indicated the area of nodule while the computer software did the quantitative analysis subsequently for each dimension. "Automated" technology that facilitates the 3D segmentation of subsolid nodule might play an important role in the future. Last, to eliminate all vessels, bronchioli and air bronchograms perfectly when performing GGN analyzing seemed not possible, and this might partly cause the interobserver variation.

In conclusion, tumor invasiveness of GGNs as defined by IASLC/ATS/ERS classification can be predicted by quantitative CT parameters. In pGGNs, CT size and one-dimensional mean CT value are determinants for tumor invasiveness. In PSNs, invasiveness can be predicted by CT size and 3D mean CT value of the nodule.

### Acknowledgements

We thank Prof. Qiang Shen from Department of Clinical Cancer Prevention, Division of Cancer Prevention and Population Sciences, The University of Texas MD Anderson Cancer Center for the language revision of this paper.

**Funding:** This work was supported by the Program of Science and Technology Commission of Shanghai Municipality 15ZR143-8200 and 16DZ2345900.

### Footnote

**Conflicts of Interest:** The authors have no conflicts of interest to declare.

**Ethical Statement:** This study was approved by the Ethics Committee of the Shanghai Chest Hospital, and the patients' written informed consent was waived by the Ethics Committee.

### References

1. Aoki T, Tomoda Y, Watanabe H, et al. Peripheral lung adenocarcinoma: correlation of thin-section CT findings with histologic prognostic factors and survival. *Radiology* 2001;220:803-9
2. Naidich DP, Bankier AA, MacMahon H, et al. Recommendations for the management of subsolid pulmonary nodules detected at CT: a statement from the Fleischner Society. *Radiology* 2013;266: 304-17.
3. Travis WD, Brambilla E, Noguchi M, et al. International association for the study of lung cancer/american thoracic society/european respiratory society international multidisciplinary classification of lung adenocarcinoma. *J Thorac Oncol* 2011;6:244-85.
4. Noguchi M, Morikawa A, Kawasaki M, et al. Small adenocarcinoma of the lung. Histologic characteristics and prognosis. *Cancer* 1995;75:2844-52.
5. Travis WD, Garg K, Franklin WA, et al. Evolving concepts in the pathology and computed tomography imaging of lung adenocarcinoma and bronchioloalveolar carcinoma. *J Clin Oncol* 2005;23:3279-87.
6. Park CM, Goo JM, Lee HJ, et al. Nodular ground-glass opacity at thin-section CT: histologic correlation and evaluation of change at follow-up. *Radiographics* 2007;27:391-408.
7. Lee SM, Park CM, Goo JM, et al. Invasive pulmonary adenocarcinomas versus preinvasive lesions appearing as ground-glass nodules: differentiation by using CT features. *Radiology* 2013;268:265-73.
8. Takahashi M, Shigematsu Y, Ohta M, et al. Tumor invasiveness as defined by the newly proposed IASLC/ATS/ERS classification has prognostic significance for pathologic stage IA lung adenocarcinoma and can be predicted by radiologic parameters. *J Thorac Cardiovasc Surg* 2014;147:54-9.
9. Landis JR, Koch GG. The measurement of observer agreement for categorical data. *Biometrics* 1977;33:159-74.
10. Yoshizawa A, Motoi N, Riely GJ, et al. Impact of proposed IASLC/ATS/ERS classification of lung adenocarcinoma: prognostic subgroups and implications for further revision of staging based on analysis of 514 stage I cases. *Mod Pathol* 2011;24:653-64.
11. Warth A, Muley T, Meister M, et al. The novel histologic International Association for the Study of Lung Cancer/American Thoracic Society/European Respiratory Society classification system of lung adenocarcinoma is a stage-independent predictor of survival. *J Clin Oncol* 2012;30:1438-46.
12. Lim HJ, Ahn S, Lee KS, et al. Persistent pure ground-glass opacity lung nodules  $\geq$  10 mm in diameter at CT scan: histopathologic comparisons and prognostic implications. *Chest* 2013;144:1291-9.
13. Takahashi S, Tanaka N, Okimoto T, et al. Long term follow-up for small pure ground-glass nodules: implications of determining an optimum follow-up period and high-resolution CT findings to predict the growth of nodules. *Jpn J Radiol* 2012;30:206-17.
14. Suzuki K, Kusumoto M, Watanabe S, et al. Radiologic classification of small adenocarcinoma of the lung: radiologic-pathologic correlation and its prognostic impact. *Ann Thorac Surg* 2006;81:413-9.
15. Honda T, Kondo T, Murakami S, et al. Radiographic and pathological analysis of small lung adenocarcinoma using the new IASLC classification. *Clin Radiol* 2013;68:e21-6.
16. Lee SM, Park CM, Goo JM, et al. Transient part-solid nodules detected at screening thin-section CT for lung cancer: comparison with persistent part-solid nodules. *Radiology* 2010;255:242-51.
17. Nakamura S, Kawata H, Nanbu R, et al. Investigation of Region of Interest (ROI) for measurement of slice thickness in Computed Tomography (CT). *Nihon Hoshasen Gijutsu Gakkai Zasshi* 2010;66:217-24.
18. Kitami A, Kamio Y, Hayashi S, et al. One-dimensional mean computed tomography value evaluation of ground-glass opacity on high-resolution images. *Gen Thorac Cardiovasc Surg* 2012;60:425-30
19. Nomori H, Ohtsuka T, Naruke T, et al. Differentiating between atypical adenomatous hyperplasia and bronchioloalveolar carcinoma using the computed tomography number histogram. *Ann Thorac Surg*

- 2003;76:867-71.
20. Ikeda K, Awai K, Mori T, et al. Differential diagnosis of ground-glass opacity nodules: CT number analysis by three-dimensional computerized quantification. *Chest* 2007;132:984-90.
  21. Yoshida J, Nagai K, Yokose T, et al. Limited resection trial for pulmonary ground-glass opacity nodules: fifty-case experience. *J Thorac Cardiovasc Surg* 2005;129:991-6.
  22. Godoy MC, Naidich DP. Subsolid pulmonary nodules and the spectrum of peripheral adenocarcinomas of the lung: recommended interim guidelines for assessment and management. *Radiology* 2009;253:606-22.

**Cite this article as:** Zhou QJ, Zheng ZC, Zhu YQ, Lu PJ, Huang J, Ye JD, Zhang J, Lu S, Luo QQ. Tumor invasiveness defined by IASLC/ATS/ERS classification of ground-glass nodules can be predicted by quantitative CT parameters. *J Thorac Dis* 2017;9(5):1190-1200. doi: 10.21037/jtd.2017.03.170